

Semiconducting  $[(\text{Bi}_4\text{Te}_4\text{Br}_2)(\text{Al}_2\text{Cl}_{6-x}\text{Br}_x)]\text{Cl}_2$  and  $[\text{Bi}_2\text{Se}_2\text{Br}](\text{AlCl}_4)$ : Cationic Chalcogenide Frameworks from Lewis Acidic Ionic LiquidsKanishka Biswas,<sup>†,‡</sup> In Chung,<sup>†</sup> Jung-Hwan Song,<sup>§</sup> Christos D. Malliakas,<sup>†</sup> Arthur J. Freeman,<sup>§</sup> and Mercouri G. Kanatzidis<sup>\*,†</sup><sup>†</sup>Department of Chemistry and <sup>§</sup>Department of Physics and Astronomy Northwestern University, Evanston, Illinois 60208, United States<sup>‡</sup>New Chemistry Unit, Jawaharlal Nehru Centre for Advanced Scientific Research, Bangalore 560064, India

## Supporting Information

**ABSTRACT:** Lewis acidic organic ionic liquids provide a novel synthetic medium to prepare new semiconducting chalcogenides,  $[(\text{Bi}_4\text{Te}_4\text{Br}_2)(\text{Al}_2\text{Cl}_{5.46}\text{Br}_{0.54})]\text{Cl}_2$  (**1**) and  $[\text{Bi}_2\text{Se}_2\text{Br}](\text{AlCl}_4)$  (**2**). Compound **1** features a cationic  $[(\text{Bi}_4\text{Te}_4\text{Br}_2)(\text{Al}_2\text{Cl}_{5.46}\text{Br}_{0.54})]^{2+}$  three-dimensional framework, while compound **2** consists of cationic layers of  $[\text{Bi}_2\text{Se}_2\text{Br}]^{2+}$ . Spectroscopically measured band gaps of **1** and **2** are  $\sim 0.6$  and  $\sim 1.2$  eV, respectively. Thermoelectric power measurements of single crystals of **1** indicate an n-type semiconductor.

Ionic liquids are special molten salts with high thermal stability, negligible vapor pressure, good ionic conductivity, and tunable solubility of both organic and inorganic compounds. They are highly promising as reactive media often referred to as fluxes for the synthesis of new materials. The use of ionic liquids in solvent extraction and organic catalysis is well-known, but their use in the synthesis of inorganic materials is relatively recent.<sup>1,2</sup> Besides classical hydrothermal/solvothermal syntheses, ionothermal syntheses have been recently employed for zeolites,<sup>3</sup> metal–organic frameworks,<sup>4</sup> clathrates,<sup>5</sup> metal nanoparticles and nanorods,<sup>6</sup> and microporous and mesoporous carbon and graphene.<sup>7,8</sup> Early examples of the synthesis of new chalcogenides in ionic liquids are  $\text{K}_4\text{Ti}_3\text{S}_{14}$ ,  $\text{KCuS}_4$ , and  $(\text{Ph}_4\text{P})\text{InSe}_{12}$ , which were crystallized out of the molten inorganic salt of  $\text{K}_2\text{S}_5$  and the organic  $(\text{Ph}_4\text{P})\text{Se}_6$ .<sup>9</sup> Although a large body of work is reported on the use of inorganic ionic liquid fluxes, metal chalcogenide chemistry in organic ionic liquids is still at an early stage. Most of the chalcogenides synthesized in ionic liquids are nanostructures of known binaries.<sup>10</sup> Recently, there have been reports of anionic molecular supertetrahedral chalcogenide clusters<sup>11</sup> and anionic open-framework selenidostannates<sup>12</sup> and  $[\text{Sn}_{36}\text{Ge}_{24}\text{Se}_{132}]^{24-}$  prepared in ionic liquids.<sup>13</sup>

Chalcogenide polycationic clusters are a rare and interesting subclass exhibiting a variety of molecular structures.<sup>14</sup> There are several methods for their synthesis, which include electrophilic and acidic media such as liquid  $\text{SO}_2$  and  $\text{H}_2\text{SO}_4$ , the use of strong oxidizing agents such as  $\text{WCl}_5$ ,<sup>15</sup>  $\text{SbF}_5$ , and  $\text{AsF}_5$ ,<sup>16</sup> or the presence of strong acceptors such as  $\text{AlCl}_3$ <sup>17</sup> and  $\text{ZrCl}_4$ .<sup>18</sup> Recently, we reported the synthesis of novel heteropolycations such as the cluster  $[\text{Sb}_7\text{S}_8\text{Br}_2]^{2+}$  and the two-dimensional frameworks of  $[\text{Bi}_2\text{Te}_2\text{Br}]^+$  and  $[\text{Sb}_2\text{Te}_2\text{Br}]^+$  using Lewis acidic ionic liquids as the reaction medium.<sup>19</sup> Ruck and co-workers also

synthesized layered polycations of  $[\text{Sb}_{10}\text{Se}_{10}]^{2+}$  in Lewis acidic ionic liquid media.<sup>20</sup> One-dimensional  $\text{Te}_4[\text{Bi}_{0.74}\text{Cl}_4]$  synthesized in ionic liquid shows interesting superconducting properties.<sup>21</sup> Cationic heterocubane  $(\text{Bi}_3\text{GaS}_5)^{2+}$  was prepared by the reaction of elemental Bi, S,  $\text{BiCl}_3$ , and  $\text{GaCl}_3$  in ionic liquid.<sup>22</sup>

Here, we report the synthesis of  $[(\text{Bi}_4\text{Te}_4\text{Br}_2)(\text{Al}_2\text{Cl}_{5.46}\text{Br}_{0.54})]\text{Cl}_2$  (**1**), a chalcogenide–halide semiconductor with extended structure of three-dimensional connectivity in an ionic liquid containing Lewis acid or strong acceptors, EMIMBr– $\text{AlCl}_3$  (EMIM = 1-ethyl-3-methylimidazolium). This is the first example of a three-dimensional polycationic chalcogenide–halide framework,  $[(\text{Bi}_4\text{Te}_4\text{Br}_2)(\text{Al}_2\text{Cl}_{5.46}\text{Br}_{0.54})]^{2+}$ , synthesized in an organic ionic liquid. We also report the discovery of  $[\text{Bi}_2\text{Se}_2\text{Br}](\text{AlCl}_4)$  (**2**), which has layered  $[\text{Bi}_2\text{Se}_2\text{Br}]^+$  cationic framework similar to previously reported  $[\text{Bi}_2\text{Te}_2\text{Br}]^+$ .<sup>19b</sup> The new compound **1** is an n-type semiconductor, as determined from Seebeck coefficient measurements.

The black needlelike crystals of compound **1** were synthesized by the reaction of elemental Bi and Te in EMIMBr– $\text{AlCl}_3$  at 165 °C for 5 days.<sup>23</sup> The crystal structure was determined from single-crystal X-ray diffraction data collected at 100 K on a STOE IPDS2 X-ray diffractometer. Compound **1** crystallizes in space group  $\text{P}\bar{1}$ .<sup>24</sup> The black platelike crystals of compound **2** were synthesized similarly by the reaction of elemental Bi with elemental Se. Compound **2** is isostructural to  $[\text{Bi}_2\text{Te}_2\text{Br}](\text{AlCl}_4)$ <sup>19b</sup> and crystallizes in  $\text{P}\bar{1}$ .<sup>25</sup>

The structure of **1** consists of a cationic three-dimensional framework of  $[(\text{Bi}_4\text{Te}_4\text{Br}_2)(\text{Al}_2\text{Cl}_{5.46}\text{Br}_{0.54})]^{2+}$  and is charge-balanced by two  $\text{Cl}^-$  anions. Figure 1 shows the structure of  $[(\text{Bi}_4\text{Te}_4\text{Br}_2)(\text{Al}_2\text{Cl}_{5.46}\text{Br}_{0.54})]^{2+}$  along the *b* axis. The structure is made of infinite layers of  $(\text{Bi}_4\text{Te}_4\text{Br}_2)^{2+}$ , which are connected in the third dimension by the neutral dimer  $\text{Al}_2\text{Cl}_{5.46}\text{Br}_{0.54}$  through Bi1–Br2 bonds [3.258(14) Å;<sup>19b,26</sup> Figure 2]. The layers of  $(\text{Bi}_4\text{Te}_4\text{Br}_2)^{2+}$  are made of parallel infinite chains of  $[\text{Bi}_2\text{Te}_2]^{2+}$ , which are connected with  $\text{Br}^-$  ions along the crystallographic *a* axis (Figure 1). The Bi–Br bridging distances are normal and range from 3.217(6) to 3.234(5) Å.<sup>19b,26</sup> The chain of  $[\text{Bi}_2\text{Te}_2]^{2+}$  consists of rhombic units of  $(\text{BiTe})_2$  having Te–Bi–Te angles ranging from 88.22(8) to 91.78(9)°. The Bi1 and Bi2 atoms are in the 3+ oxidation state and are 5-fold-coordinated by three Te and two bridging Br atoms to form a distorted square-

Received: March 29, 2013

Published: April 29, 2013

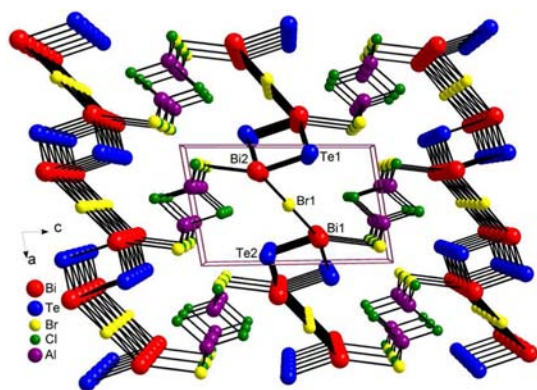


**Figure 1.** Crystal structure of a three-dimensional framework of  $[(\text{Bi}_4\text{Te}_4\text{Br}_2)(\text{Al}_2\text{Cl}_{5.46}\text{Br}_{0.54})]^{2+}$ , viewed along the  $b$  axis.

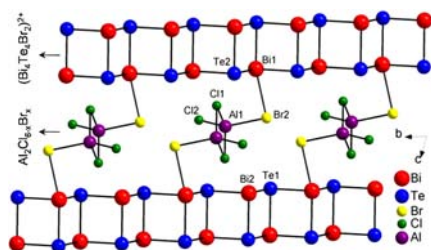


**Figure 2.** Crystal structure of  $[(\text{Bi}_4\text{Te}_4\text{Br}_2)(\text{Al}_2\text{Cl}_{5.46}\text{Br}_{0.54})]^{2+}$ , showing the  $(\text{Bi}_4\text{Te}_4\text{Br}_2)^{2+}$  slab and the linking dimer of  $\text{Al}_2\text{Cl}_{5.46}\text{Br}_{0.54}$  which connects the slabs via Bi–Br bonds [3.258(14) Å].

pyramidal geometry. The Bi–Te bond lengths range from 2.9475(8) to 2.9779(8) Å.

It is worth noting that the neutral dimer  $\text{Al}_2\text{Cl}_{5.46}\text{Br}_{0.54}$  is stabilized inside the framework of compound **1** (Figure 2). Generally, the dimer of  $\text{AlCl}_3$  i.e.,  $\text{Al}_2\text{Cl}_6$ , exists either in melts or in the gas phase. The related dimer  $\text{Al}_2\text{Cl}_{5.46}\text{Br}_{0.54}$  resides between two layers of  $(\text{Bi}_4\text{Te}_4\text{Br}_2)^{2+}$  and acts as a pillar through Br atoms. In  $\text{Al}_2\text{Cl}_{5.46}\text{Br}_{0.54}$ , moderately distorted tetrahedra are connected through chloride bridges to form a dimer, in which the Al–Cl and Al–Br bond lengths range from 2.056(13) to 2.414(4) and 2.752(14) Å, respectively, and the Cl–Al–Cl angle ranges from 103.9(5) to 120.6(4)°. Two nonbonded Cl4 atoms responsible for charge neutrality are located between the  $(\text{Bi}_4\text{Te}_4\text{Br}_2)^{2+}$  slabs.

Thermogravimetric analysis (TGA) under a  $\text{N}_2$  atmosphere (Figure S2, Supporting Information, SI) shows that compound **1** starts to lose weight at  $\sim 400$  K and undergoes a sharp weight loss at 630 K. This weight loss is attributed to  $\text{AlCl}_3$  and  $\text{Al}_2\text{Cl}_{6-x}\text{Br}_x$  and leads to  $\text{Bi}_2\text{Te}_3$  as the final residue, as judged by powder X-ray diffraction (PXRD) after TGA (Figure S2, SI). Differential thermal analysis (DTA) indicates an endothermic event at  $\sim 657$  K (Figure S3, SI). The PXRD pattern measured after DTA indicates a pure  $\text{Bi}_2\text{Te}_3$  phase (Figure S3, SI) and suggests incongruent melting for compound **1**.

Compound **1** is a narrow-gap semiconductor. Its electronic absorption spectrum shows an absorption edge of  $\sim 0.6$  eV (Figure 3a), consistent with the black color. The absorption rise is not sharp and is suggestive of an indirect gap. This is consistent with the results of the electronic structure calculations presented below. The band gap is lower than that of the previously reported two-dimensional compound  $[\text{Bi}_2\text{Te}_2\text{Br}](\text{AlCl}_4)$  ( $E_g \sim 0.8$  eV),<sup>19b</sup> and this is attributed to the fact that its structure is three-dimensional. The band gap of **2** is  $\sim 1.2$  eV (Figure 3a).

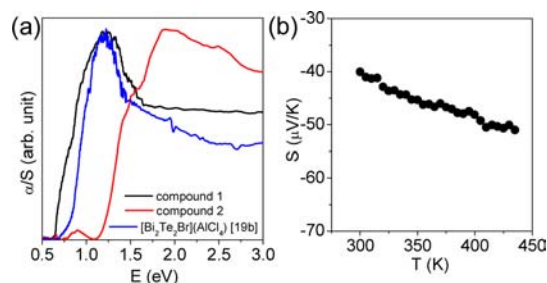


**Figure 3.** (a) Electronic absorption spectra of compounds **1**, **2**, and  $[\text{Bi}_2\text{Te}_2\text{Br}](\text{AlCl}_4)$ .<sup>19b</sup> (b) Temperature-dependent Seebeck coefficient ( $S$ ) measured on single crystals of compound **1**.

The Seebeck coefficient ( $S$ ) measured on a single-crystal sample of compound **1** at 300 K was  $\sim -40$   $\mu\text{V}/\text{K}$ , which increased to  $\sim -52$   $\mu\text{V}/\text{K}$  at 435 K (Figure 3b). The negative sign indicates the presence of n-type carriers. The room temperature resistivity is mildly anisotropic. It was measured as  $\sim 156$   $\Omega$  cm along the crystallographic  $b$  direction, while along the perpendicular direction, it was  $\sim 500$   $\Omega$  cm (Figure S4, SI).

In order to understand the optical absorption and transport properties, the electronic band structure of compound **1** was calculated using the full potential linearized augmented plane wave method with the screened-exchange local density approximation (sX-LDA) and the Hedin–Lundqvist (LDA) forms of the exchange–correlation potential.<sup>19</sup> Figure 4a shows

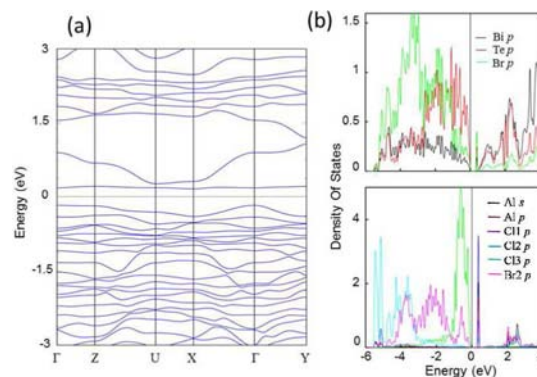


**Figure 4.** (a) Electronic band structure of **1** and (b) projected angular-momentum-resolved DOS for the individual elements. The upper and lower panel in part b represents the DOS for the individual elements in  $(\text{Bi}_4\text{Te}_4\text{Br}_2)^{2+}$  and  $\text{Al}_2\text{Cl}_{5.46}\text{Br}_{0.54}$ .

the electronic band structure of compound **1**. The valence band maximum (VBM) is located at the  $\Gamma$  point. Near the conduction band minimum (CBM), there is a very flat band that is well separated from the dispersive conduction bands. It is expected that the flat band at the CBM contributes significantly to n-type transport because of its presumed massive carriers. Its isotropic and nondispersive characteristics imply that, if the n-type carriers dominate, the measurement of the resistivity should show only a small difference along different orientations. Also, the resistivity should be relatively large compared to the layered compound,  $[\text{Bi}_2\text{Te}_2\text{Br}](\text{AlCl}_4)$ ,<sup>19b</sup> which is indeed supported by the measured resistivity values.

sX-LDA calculations with spin–orbit interaction included gives a direct band gap of 0.33 eV, which is smaller than the experimentally measured value of  $\sim 0.6$  eV. The projected angular-momentum-resolved density of states (DOS) in Figure 4b reveals that the dispersive characteristics in the band

structure mainly originate from the significant p–p mixing effect between Bi, Te, and Br atoms. The largest contribution to the flat band at the CBM comes from the Al–Cl1 bonds, as shown in the DOS in Figure 4b. The very narrow bandwidth can be accounted for by the localized nature of the molecular fragment of  $\text{Al}_2\text{Cl}_{5.46}\text{Br}_{0.54}$ . The molecular fragment creates this band, which is more reminiscent of an impurity level in a semiconductor than a bona fide conduction band. In essence, the functional conduction band in the material can be considered to be the dispersed band with a minimum, the U point. This band is composed mainly of empty Te and Bi p states in the framework. Therefore, the optical transition observed in the electronic absorption spectra of Figure 3a is indirect in nature. The electronic excitation is from essentially filled Te orbitals from the top of the VBM at the  $\Gamma$  point to the CBM at the U point.

The atoms Cl2, which have a Bi neighbor at 3.220(10) Å, have strong covalent characteristics and show a large and broad contribution to much deeper energy levels (–6 to –3 eV below the VBM) compared to Cl3. The Cl3/Br2 in  $\text{Al}_2\text{Cl}_{5.46}\text{Br}_{0.54}$  contributes to the energy levels near the VBM and shows pronounced peaks due to its strong ionic characteristics. More importantly, the disordered Br2 in  $\text{Al}_2\text{Cl}_{5.46}\text{Br}_{0.54}$  which has an atomic environment similar to that of Cl2, has an even broader contribution to the valence bands, as shown in Figure 4b, again via hybridization with Bi states. This is also illustrated in Figure S5 in the SI, which shows that the charge densities along the Bi–Br2 bonding axis are relatively large compared to those of Bi–Cl2. The Br plays an important role in making a covalent bond bridge between  $(\text{Bi}_4\text{Te}_4\text{Br}_2)^{2+}$  and  $\text{Al}_2\text{Cl}_{5.46}\text{Br}_{0.54}$ .

The new compounds **1** and **2** have unusual cationic chalcogenide frameworks and can be synthesized in a Lewis acidic ionic liquid. The mild reaction conditions and solubility of various elements in ionic liquids are unique media that allow the synthesis of new kinetically stable solids. Thus, organic Lewis acidic ionic liquids provide a generalized synthetic pathway toward polycationic chalcogenide frameworks.

## ■ ASSOCIATED CONTENT

### Supporting Information

Experimental section and characterization and structural details including CIF files of compounds **1** and **2**. This material is available free of charge via the Internet at <http://pubs.acs.org>.

## ■ AUTHOR INFORMATION

### Corresponding Author

\*E-mail: m-kanatzidis@northwestern.edu.

### Notes

The authors declare no competing financial interest.

## ■ ACKNOWLEDGMENTS

Financial support from the National Science Foundation (Grant DMR-1104965) is gratefully acknowledged.

## ■ REFERENCES

(1) (a) Antonietti, M.; Kuang, D.; Smarsly, B.; Zhou, Y. *Angew. Chem., Int. Ed.* **2004**, *43*, 4988. (b) Freudenmann, D.; Wolf, S.; Wolff, M.; Feldmann, C. *Angew. Chem., Int. Ed.* **2011**, *50*, 11050.  
 (2) Ma, Z.; Yu, J.; Dai, S. *Adv. Mater.* **2010**, *22*, 261.  
 (3) Morris, R. E. *Angew. Chem., Int. Ed.* **2008**, *47*, 442.  
 (4) For example, see: (a) Dybtsev, D. N.; Chun, H.; Kim, K. *Chem. Commun.* **2004**, 1594. (b) Lin, Z.; Slawin, A. M. Z.; Morris, R. E. *J. Am. Chem. Soc.* **2007**, *129*, 4880.

(5) Guloy, A. M.; Ramlau, R.; Tang, Z.; Schnelle, W.; Baitinger, M.; Grin, Y. *Nature* **2006**, *443*, 320.

(6) For example, see: (a) Dupont, J.; Fonseca, G. S.; Umpierre, A. P.; Fichtner, P. F. P.; Teixeira, S. R. *J. Am. Chem. Soc.* **2002**, *124*, 4228. (b) Itoh, H.; Naka, K.; Chujo, Y. *J. Am. Chem. Soc.* **2004**, *126*, 3026. (c) Migowski, P.; Dupont, J. *Chem.—Eur. J.* **2007**, *13*, 32. (d) Wang, Y.; Yang, H. *J. Am. Chem. Soc.* **2005**, *127*, 5316.

(7) Lee, J. S.; Wang, X.; Luo, H.; Baker, G. A.; Dai, S. *J. Am. Chem. Soc.* **2009**, *131*, 4596.

(8) Lu, J.; Yang, J.-X.; Wang, J.; Lim, A.; Wang, S.; Loh, K. P. *ACS Nano* **2009**, *3*, 2367.

(9) (a) Kanatzidis, M. G.; Sutorik, A. C. *Prog. Inorg. Chem.* **1995**, *43*, 151. (b) Chondroudis, K.; McCarthy, T. J.; Kanatzidis, M. G. *Inorg. Chem.* **1996**, *35*, 840. (c) Dhingra, S.; Kanatzidis, M. G. *Science* **1993**, *258*, 1769.

(10) (a) Biswas, K.; Rao, C. N. R. *Chem.—Eur. J.* **2007**, *13*, 6123. (b) Ma, J.; Duan, X.; Lian, J.; Kim, T.; Peng, P.; Liu, X.; Liu, Z.; Li, H.; Zheng, W. *Chem.—Eur. J.* **2010**, *16*, 13120. (c) Ma, J.; Liu, Z.; Lian, J.; Duan, X.; Kim, T.; Peng, P.; Liu, Z.; Chen, Q.; Yao, G.; Zhen, W. *CrystEngComm* **2011**, *13*, 3072.

(11) Xiong, W.-W.; Li, J.-R.; Hu, B.; Tan, B.; Li, R. F.; Huang, X. Y. *Chem. Sci.* **2012**, *3*, 1200.

(12) (a) Li, J.-R.; Xie, Z.-L.; He, X.-W.; Li, L.-H.; Huang, X.-Y. *Angew. Chem., Int. Ed.* **2011**, *50*, 11395. (b) Lin, Y.; Dehnen, S. *Inorg. Chem.* **2011**, *50*, 7913.

(13) Lin, Y.; Massa, W.; Dehnen, S. *J. Am. Chem. Soc.* **2012**, *134*, 4497.

(14) Brownridge, S.; Krossing, I.; Passmore, J.; Jenkins, H. D. B.; Roobottom, H. K. *Coord. Chem. Rev.* **2000**, *197*, 397.

(15) Beck, J.; Wetterau, J. *Inorg. Chem.* **1995**, *34*, 6202.

(16) Klapötke, T.; Passmore, J. *Acc. Chem. Res.* **1989**, *22*, 234.

(17) Beck, J.; Dolg, M.; Schlüter, S. *Angew. Chem., Int. Ed.* **2001**, *40*, 2287.

(18) Beck, J.; Hedderich, S. *J. Solid State Chem.* **2003**, *172*, 12.

(19) (a) Zhang, Q.; Chung, I.; Jang, J. I.; Ketterson, J. B.; Kanatzidis, M. G. *J. Am. Chem. Soc.* **2009**, *131*, 9896. (b) Biswas, K.; Zhang, Q.; Chung, I.; Song, J.-H.; Androulakis, J.; Freeman, A. J.; Kanatzidis, M. G. *J. Am. Chem. Soc.* **2010**, *132*, 14760.

(20) Ahmed, E.; Isaeva, A.; Fiedler, A.; Haft, M.; Ruck, M. *Chem.—Eur. J.* **2011**, *17*, 6487.

(21) Ahmed, E.; Beck, J.; Daniels, J.; Doert, T.; Eck, M. S.; Heerwig, A.; Isaeva, A.; Lidin, S.; Ruck, M.; Schnelle, W.; Stankowski, A. *Angew. Chem., Int. Ed.* **2012**, *51*, 8106.

(22) Freudenmann, D.; Feldmann, C. *Dalton Trans.* **2011**, *40*, 452.

(23) Synthesis of **1**: Amounts of 52.5 mg (0.25 mmol) of elemental Bi metal, 96 mg (0.75 mmol) of elemental Te metal, 250 mg (1.87 mmol) of anhydrous  $\text{AlCl}_3$  (Sigma-Aldrich, 99.99%), and 75 mg (0.39 mmol) of EMIMBr were loaded into a 20 mL glass vial inside a glovebox. The vial was closed and put in a preheated oven at 165 °C for 5 days. After completion of the reaction, the vial was opened inside the glovebox and the product was washed with chloroform. Black needlelike crystals were obtained with 74% yield.

(24) X-ray crystal data for **1** at 100(2) K: STOE IPDS2 diffractometer, Mo  $K\alpha$  radiation, monoclinic;  $P\bar{1}$ ;  $Z = 1$ ;  $a = 6.9660(6)$  Å,  $b = 8.4658(7)$  Å,  $c = 11.4626(10)$  Å,  $\alpha = 68.343(7)^\circ$ ,  $\beta = 75.142(7)^\circ$ ,  $\gamma = 72.289(7)^\circ$ ;  $V = 590.50(9)$  Å<sup>3</sup>. Collection and refinement data:  $2\theta_{\text{max}} = 58.32^\circ$ ;  $d_{\text{calc}} = 5.265$  g/cm<sup>3</sup>;  $F(000) = 784$ ; 5769 total reflections; 2940 unique reflections [ $F_o^2 > 2\sigma(F_o^2)$ ]; 96 parameters; GOF = 0.969;  $R1 = 5.27\%$  and  $wR2 = 11.77\%$  for  $I > 2\sigma(I)$ .

(25) X-ray crystal data for **2** at 100(2) K: monoclinic;  $P\bar{1}$ ;  $Z = 2$ ;  $a = 6.8705(9)$  Å,  $b = 8.2425(10)$  Å,  $c = 11.4800(15)$  Å,  $\alpha = 69.096(9)^\circ$ ,  $\beta = 73.458(10)^\circ$ ,  $\gamma = 72.469(9)^\circ$ ;  $V = 567.54(13)$  Å<sup>3</sup>. Collection and refinement data:  $2\theta_{\text{max}} = 58^\circ$ ;  $d_{\text{calc}} = 4.825$  g/cm<sup>3</sup>;  $F(000) = 700$ ; 5472 total reflections; 2791 unique reflections [ $F_o^2 > 2\sigma(F_o^2)$ ]; 95 parameters; GOF = 1.024;  $R1 = 5.89\%$  and  $wR2 = 15.66\%$  for  $I > 2\sigma(I)$ .

(26) (a) Battagila, L. P.; Corradi, A. B. *J. Chem. Soc., Dalton Trans.* **1990**, 1675. (b) Robertson, B. K.; McPherson, W. G.; Meyers, E. A. *J. Phys. Chem.* **1967**, *71*, 3531.